A Computational Model of the Canine Pulmonary Veins Sleeves

Chu-Pin Lo Tzyy-Leng Horng [1,*] Hsiang-Ning Luk[2] Hui-Chun Tien

Juan-Ming Yuan Daniel Lee[3]

Department of Applied Mathematics, Providence University, Taichung, Taiwan, 433 ROC
[1]*Department of Applied Mathematics, Feng Chia University, Taichung, Taiwan, 407 ROC*
[2]*Department of Anesthesiology, Taichung Veterans General Hospital, Taichung, Taiwan, 407 ROC*
[3]*Department of Mathematics, Tunghai University, Taichung, Taiwan, 407 ROC*

Received 2 July 2006; Accepted 15 Aug 2006

Abstract

The cellular electrophysiological properties of the pulmonary vein sleeves (PVS), the intersection between pulmonary veins and left atrium, were reported few decades ago. However, the clinical significance of pulmonary vein sleeves was not found until recently. In patients with atrial fibrillation, it was found that ectopic foci existed in the pulmonary vein sleeves. Therefore, electrophysiological studies on PVS have drawn a lot of attention recently. For example, in the experiments of dogs and rabbits, besides the fast response type of action potential, various pacemaker-like automaticities and triggered activities, e.g., early afterdepolarizations (EAD), delayed afterdepolarizations (DAD), have been demonstrated in the PVS under physiological or pathophysiological situations [3-14, 16-18]. In this study, we have developed a mathematical model which fits well the experiments for the canine PVS in [17]. Using this model, besides the normal response of the PVS cells we have also successfully reproduced the experimentally observed frequency responses and ischemia/hyperkalemia phenomena.

Keywords: Pulmonary vein sleeves, Action potential

Introduction

Pulmonary veins (PV) are the great vessels connected between lung and left atrium and transport oxygenated blood to the heart. There are 4 pulmonary veins in human beings. At the intersection between pulmonary veins and left atrium, there is a short segment covered with striated cardiac muscle (not smooth muscle) and called pulmonary vein sleeve (PVS). Complex anatomical architecture of the mammalian PVS, due to the intermingled circular and longitudinal muscular bundles, might contribute to formation of ectopic focus/foci during atrial tachyarrhythmias. Any changes in the action potentials parameters of PV sleeves myocytes are prone to cause abnormal impulse formation and conduction. Arrhythmias can be generated by the mechanisms such as abnormal automaticity, triggered activity and reentry. On the cellular mechanisms responsible for the normal and abnormal electrophysiological properties of PV sleeves myocytes, various transmembrane ionic currents and intracellular ionic activities are involved.

The role of pulmonary vein (PV) sleeves in humans is not clear until recently. It has been demonstrated in a pioneer work from Haissaguerre et al. [1] that ectopic focus/foci originated in pulmonary vein (PV) have been mapped and ablated in patients with focal atrial fibrillation. Atrial tachyarrhythmias could therefore be successfully terminated and sinus rhythm could be resumed. A great attention on the role of PV in initiating and sustaining focal atrial fibrillation therefore has been drawn. In literature, fundamental characterization of PV sleeves has been documented in rodents [2], dogs and rabbits [3-18]. In addition to fast-response action potentials, spontaneous activities and triggered activities, such as early afterdepolarization (EAD) and delayed afterdepolarization (DAD) have also been shown. In Chen et al. series of papers, it has been reported that a high incidence of pacemaker cells activity, EAD, DAD, and so-called high frequency irregular rhythms of the multicellular preparations or isolated single myocytes from PV sleeves from normal healthy dogs and rabbits. Based on the cellular electrophysiological data, Chen et al. therefore made a conclusion that PV sleeves contained multiple types of cardiomyocytes with distinct electrophysiological characteristics and implied a role of PV in initiating atrial fibrillation. However, the other five international independent research groups have presented a

* Corresponding author: Tzyy-Leng Horng
Tel: +886-4-24517250 ext. 5126; Fax: +886-4-4510801
E-mail: allen.horng@msa.hinet.net

contradictory conclusion. Namely, no abnormal automaticity or triggered activity was ever found in dogs and rabbits pulmonary veins sleeves under normal experimental conditions. Therefore, this controversy regarding the important electrophysiological properties of pulmonary veins sleeves need a thorough re-examination in details.

Since the pioneering work of Hodgkin and Huxley [19] in describing quantitatively the ionic currents of the squid giant axon, mathematical models have provided one important and useful approach to study the cardiac cells. Mathematical algorithms and equations are derived to describe versatile action potentials configurations, transmembrane ionic currents and channels, pumps, exchangers and intracellular ions activities under normal and abnormal conditions. In literature, there have appeared many mathematical models for the various types of cells in heart of different species. However there are no suitable computational models for the PV sleeves until now. Since the important role of the PV sleeves and the debate mentioned above, it is urgent and valuable to build up a mathematical model for the PV sleeves.

In the present paper, based on the experimental data in [17], we have established a mathematical model to explore various canine PVS electrophysiological characteristics, under both normal and pathological conditions.

Materials and Methods

Establishment of the canine PV sleeves mathematical model

In the literature, there are no specific mathematical models for the PV. We will modify the mathematical model for the canine right atrium in [20] and [21] to serve our purpose. As stated in [13] and [22], there are no differences in kinetic or voltage-dependent properties of currents between the right atrium (RA), left atrium (LA), and PV. The only difference is the magnitude of some ion current densities, which then causes characteristic changes of the action potential. In summary, LA myocytes have larger rapid delayed rectifier current I_{Kr} than do RA. Therefore, the action potential duration (APD) is shorter in the LA versus RA and the effective refractory period is also shorter in the LA compared with RA, resulting in faster repolarization in LA. On the other hand, PV has greater rapid and slow delayed rectifier currents, I_{Kr}, I_{ks}, respectively and smaller inward rectifier current I_{K1}, transient outward K^+ current I_{to}, and L-type Ca^{2+} current I_{Ca}. Hence, PV has shorter APD, more positive resting membrane potential (RMP), and slower phase 0 upstroke velocity, compared to LA.

Since the differences of electrophysiological properties between RA and PV are not essential from the kinetics viewpoint as mentioned above, we will modify the model in [20, 21] by mainly adjusting the current densities according to the experimental data in [17].

Parameters of the model

All of the model equations of this study are the same as in [21], except for some revisions in the appendix. All of the parameters in our model are chosen in Table 1 of [21] except those indicated below. The initial data are taken from Table 1 of [20]. Since the experimental samples in [17] are superfused with the normal Tyrode solution composed of (mM), *NaCl* 130, *KCl* 4, $CaCl_2$ 1.8*;* $MgCl_2$ 0:5*;*$NaHCO_3$ 12*;* and glucose 5, the extracellular ionic concentrations are fixed as: potassium concentration $[K^+]_o$ = 4 mM*;* chloride concentration $[Cl^-]_o$ = 138.6 mM*;* sodium concentration $[Na^+]_o$ = 142 mM*;* calcium concentration $[Ca^{2+}]_o$ =1.8 mM*:* As explained in [20], the maximal conductance of the transient outward *K*+ current, g_{to}, was changed to 0.04956 nS/pF.

Table 1. Parameters of action potentials under different pacing rates.

Pacing frequency (Hz)	Vmax (V/s)	RMP (mV)	APD90 (ms)	APA (mV)
0.05	58.19235	-83.5423	206.3	116.3847
0.1	58.266	-83.2615	209	116.532
0.5	55.342952	-80.9603	211.9	116.2202
1	57.65065	-78.864	211.3	115.3013
2	56.8262	-76.9254	207.6	113.6524
3	53.66565	-75.2937	200.67	107.3313
4	40.966124	-71.4587	186.9	85.6192

In order to fit the experimental results in [17], we have reasonably revised some ionic current conductance in Table 1 of [21]; see the section "Results" below.

ODE numerical method

Here we used MATLAB function ODE15S as the ODE solver. ODE15S is a stiff multistep variable order solver based on the numerical differentiation formulas (NDFs). Optionally, it uses the backward differentiation formulas (BDFs, also known as Gear's method) that are usually less efficient. It turns out to be very cost efficient for our current stiff problem.

Results and Discussion

We used the current-clamp mode with stimulus current intensity I_{stim} =-2900*pA*, duration=2 ms to record the action potential and various current densities. To describe the action potential more precisely, usually the following parameters will be measured: the action potential amplitude(*APA*), resting membrane potential(*RMP*), action potential duration (*APD*) at 50% and 90% of repolarization (APD_{50} and APD_{90}, respectively), and the maximal velocity of depolarization of phase 0 ($V_{\max}$).

Frequency response of the action potential

Using our canine PV model with rapid delayed rectifier current conductance and inward rectifier current conductance gK_r = 0.055872*;* gK_1 = 0.06 (nS/pF), respectively, we repeated the frequency response experiment as in [17]. The computer simulation results under the pacing rates (Hz): 0.05, 0.1, 0.5, 1, 2, 3, 4, are shown in Figure 1, 2, 3, and Table 1. We then conclude that the action potentials become shorter (*APD* ↘), depolarized (*RMP* ↗) and depressed (*V*max ↘) as the frequency increases, which are consistent with the experimental results in [17] (see Figure 3 therein). The above phenomena of rate adaptation can be explained as follows. When the pacing frequency increases, less amount of potassium current flows out of the cell before the next stimulus, which induces depolarized RMP. Therefore, fast sodium current inactivates as RMP increases due to the voltage-dependent inactivation (see Figure 2 in the reference [7] of [21]), which causes depressed

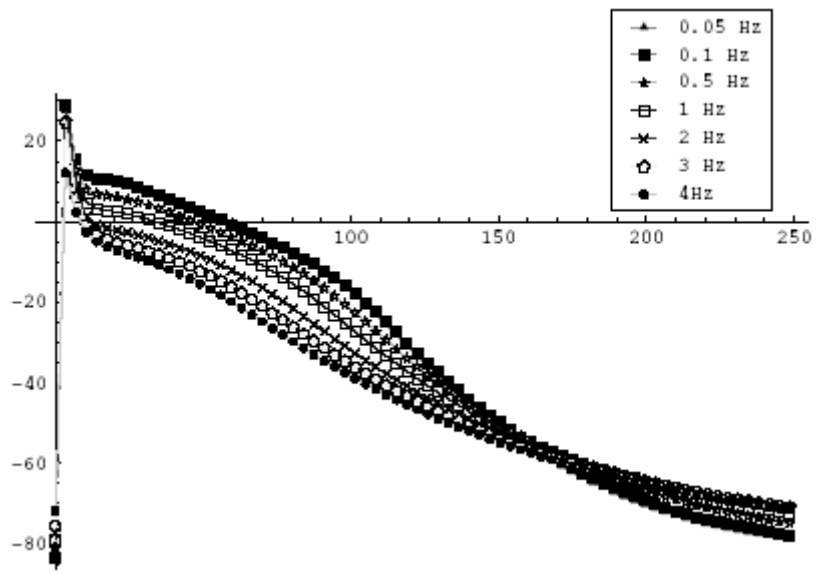

Figure 1. Frequency response of action potential under different pacing rates.

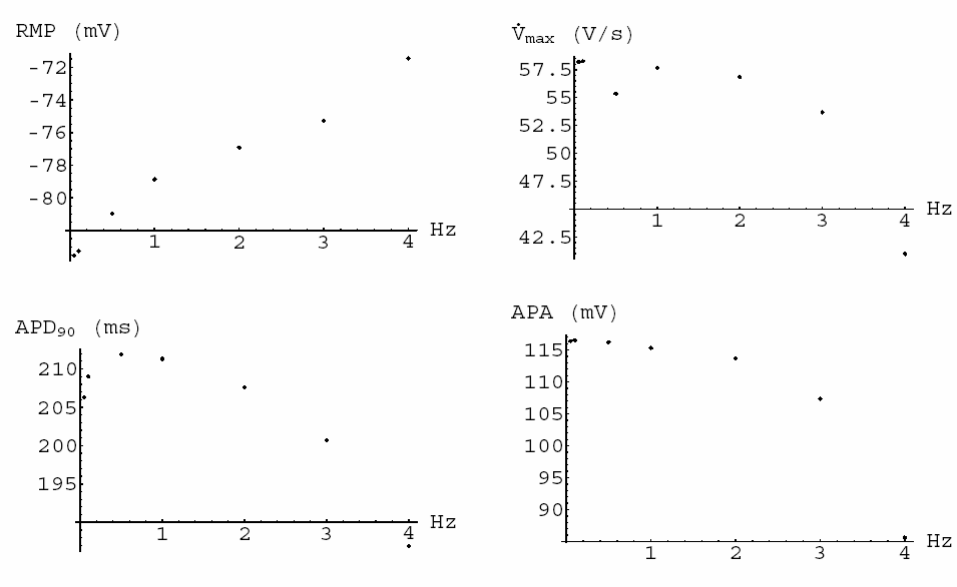

Figure 2. Parameters of action potentials under different pacing rates.

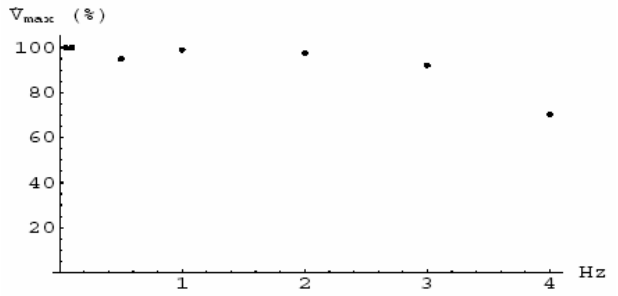

Figure 3. Vmax versus frequency (normalized).

velocity of upstroke. As stated in [21], the voltage dependent and Ca^{2+}-dependent inactivation of the L type calcium channel under depolarized RMP account for the reduced APD. The plot of diastolic time interval versus action potential duration is the well-known APD restitution curve which is an important judgement index for fibrillation [23-25].

Ischemia/hyperkalemia

Myocardial ischemia results from a withdrawal of oxygen from myocardial tissue (due to inefficient or absent perfusion), resulting in disturbances to aerobic respiration and ATP production. Alterations in intracellular ATP can alter the activity of membrane pumps, and thus the distribution of critical ions, *e.g.*, Na^+ and K^+. As the intracellular stores of ATP diminish due to reduced aerobic respiration, Na^+ /K^+ pumps responsible for ion distribution also demonstrate reduced activity. Though normally this pump acts to relocate sodium out of the cell and potassium into the cell, a lethargic pump performs this process inefficiently.

Thus, there is an extracellular accumulation of the potassium, referred to as "*hyperkalemia*". We mimicked the hyperkalemia situation by varying the extracellular potassium

Table 2. Parameters of action potentials under different extracellular potassium concentrations.

$[K^+]_o$ (mM)	V_{max} (V/s)	RMP (mV)	APD_{90} (ms)	APA (mV)
0.4	43	-105	448.1	129
1	45	-102	317.4	126
4	58	-80	212.8	116
8	41.5	-65	181.2	83
12	32	-57.5	173.6	64
16	0	-55	0	0

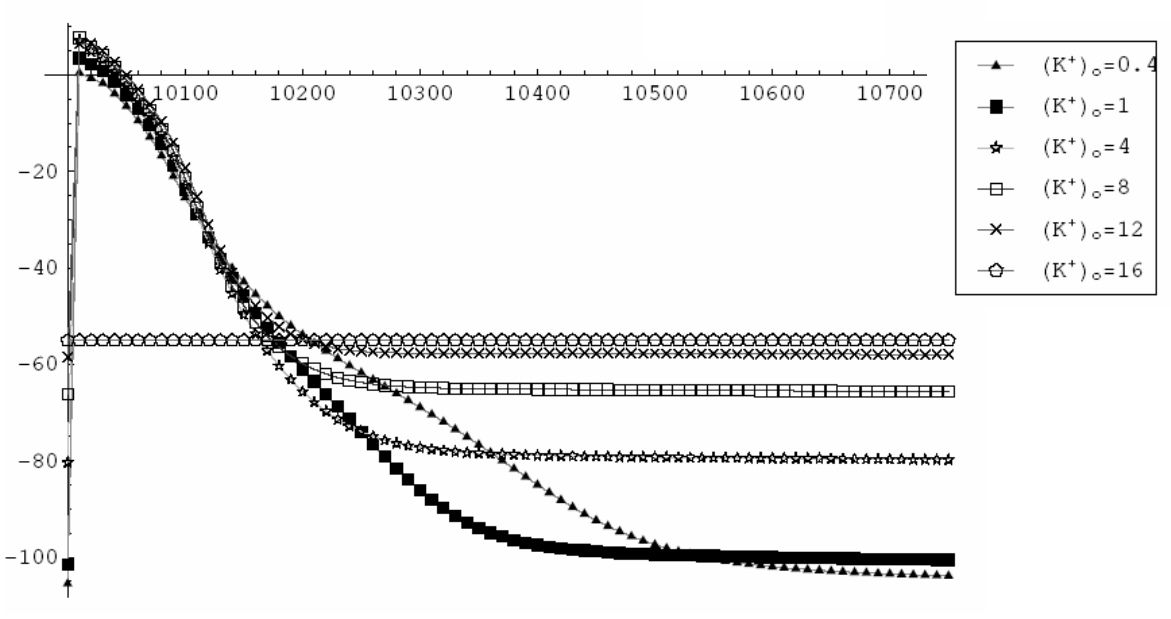

Figure 4. Action potentials under different extracellular potassium concentrations

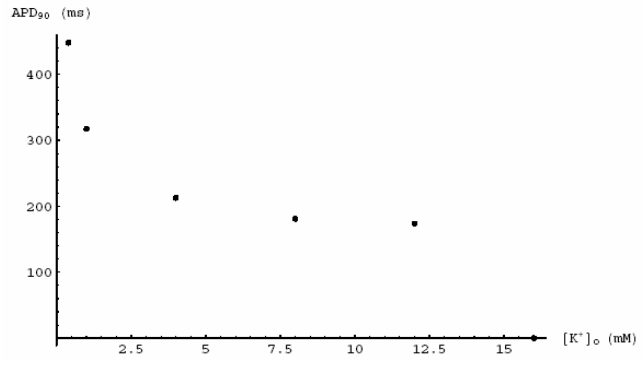

Figure 5. APD90 versus [K+]o.

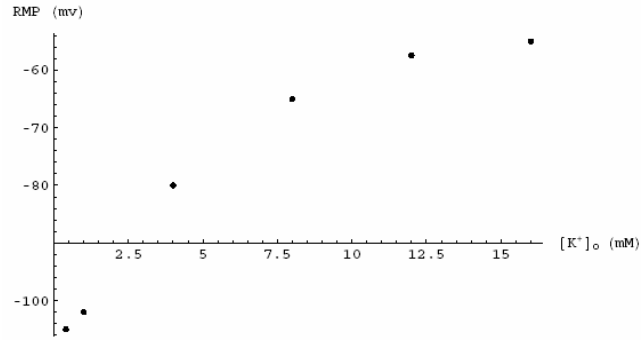

Figure 6. RMP versus [K+]o.

concentration as in [17]. The obtained results are shown in Figures 4, 5, 6, 7 and Table 2. Clearly, with the increased extracellular potassium, RMP becomes more positive, increasing sodium channel inactivation and reducing the inward sodium current. This dominating effect is somewhat mitigated by the increased RMP being closer to the action potential threshold.

Thus, moderate increases (0.4 mM to 4 mM) in potassium may actually increase upstroke velocity V_{max} (this is termed "*superconduction*"), while large increases in extracellular potassium concentrations (>4mM) begin to inactivate the sodium current and decrease upstroke velocity. In summary, our simulation results have demonstrated the classical characteristics of ischemic cells: depolarization of resting potential, reduced action potential upstroke, reduced conduction velocity, and reduced action potential duration, which were consistent with the experimental results in [17] (see Figures 4 therein).

Conclusions

In this study, we have successfully reproduced the key characteristics of the experiments in [17] about frequency response and varying extracellular potassium concentration.

$$\frac{dV}{dt} = -I_{ion} - \frac{I_{stim}}{Cm} \tag{rA1}$$

$$I_{ion} = I_{Na} + I_{K1} + I_{to} + I_{Kur,d} + I_{Kr} + I_{Ks} + I_{Ca} + I_{Cl,Ca} + I_{p,Ca} + I_{NaCa} + I_{NaK} + I_{b,Na} + I_{b,Ca} + I_{b,Cl} = 0.0018(V - E_{Cl}) \quad \text{(See (2), (4) of [20])} \tag{rA2}$$

$$\frac{d[Na^+]_i}{dt} = \frac{C_m(-3I_{Nak} - 3I_{NaCa} - I_{b,Na} - I_{Na} + CT_{NaCl})}{FVi}, \tag{rA3}$$

$$\text{where } CT_{NaCl} = 0.115\left(\frac{87.8251}{E_{Na} - E_{Cl} + 87.8251}\right) \quad \text{(see (3) of [20])}$$

$$\frac{d[K^+]_i}{dt} = \frac{C_m(2I_{Nak} - I_{K1} - I_{to} - I_{Kur,d} - I_{Kr} - I_{Ks}) - I_{stim})}{FVi} \tag{rA4}$$

$$\frac{d[Cl^-]_i}{dt} = \frac{C_m(I_{Cl,Ca} + I_{b,Cl} + CT_{NaCl})}{FVi} \tag{rA5}$$

$$\frac{d[Ca^{2+}]_i}{dt} = \frac{C_m(2I_{NaCa} - I_{p,Ca} - I_{Ca} - I_{b,Ca})}{2FVi} + \frac{V_{up}(I_{up,leak} - I_{up}) + V_{rel}I_{rel})}{Vi} - \frac{d[Ca^{2+}]_{Trpm}}{dt} - \frac{d[Ca^{2+}]_{Cmdn}}{dt} \tag{rA6}$$

$$\frac{d[Ca^{2+}]_{rel}}{dt} = I_{tr} - I_{rel} - \frac{d[Ca^{2+}]_{Csqn}}{dt} \tag{rA8}$$

$$I_{K1} = \sqrt{\frac{[K^+]_O}{5.4}}\,\frac{gK1(V - E_K)}{1 + \exp[0.07(V + 80)]} \tag{rA19}$$

$$I_{to} = 0.04956O_a^3O_i(V - E_K) \tag{rA20}$$

$$I_{Kur,d} = 0.75\left(0.00855 + \frac{0.0779}{1 + \exp\left(\frac{V + 11}{-16}\right)}\right)U_a^3U_i(V - E_K) \tag{rA29}$$

$$g_{Kur,d} = 0.75\left(0.00855 + \frac{0.0779}{1 + \exp\left(\frac{V + 11}{-16}\right)}\right) \tag{rA30}$$

$$I_{Kr} = \sqrt{\frac{[K^+]_O}{5.4}}\,g_{KrXr}\left(0.07 + \frac{0.58}{1 + \exp[(V + 15)/22.4]}\right)(V - E_K) \tag{rA39}$$

$$\frac{1}{[C_{mdn}]_{\max}}\frac{d[Ca^{2+}]C_{mdn}}{dt} = 200[Ca^{2+}]_i\left(1 - \frac{[Ca^{2+}]C_{mdn}}{[C_{mdn}]_{\max}}\right) - 0.476\frac{[Ca^{2+}]C_{mdn}}{[C_{mdn}]_{\max}} \tag{rA74}$$

$$\frac{1}{[T_{rpn}]_{\max}}\frac{d[Ca^{2+}]T_{rpn}}{dt} = 784[Ca^{2+}]_i\left(1 - \frac{[Ca^{2+}]T_{rpn}}{[T_{rpn}]_{\max}}\right) - 0.392\frac{[Ca^{2+}]T_{rpn}}{[T_{rpn}]_{\max}} \tag{rA75}$$

$$\frac{1}{[C_{sqn}]_{\max}}\frac{d[Ca^{2+}]C_{sqn}}{dt} = 0.48[Ca^{2+}]_{rel}\left(1 - \frac{[Ca^{2+}]C_{sqn}}{[C_{sqn}]_{\max}}\right) - 0.4\frac{[Ca^{2+}]C_{sqn}}{[C_{sqn}]_{\max}} \tag{rA76}$$

As a robust computational model, this model should be tested by more pathophysiological experiments, e.g., ischemia/hypoxia, drugs effect ... Maybe new currents will be included to fit new experimental data, e.g., ATP related potassium current... In particular, the reasons leading to the automaticity phenomena and triggered waves, the main conflict in the literature, should be explored in the future works

Appendix

In this study, all of the model equations are the same as in [21], except the followings. The equation labelled “rA*” in this appendix means the revision of the equation “rA*” in [21]. Note that the revised equations (rA2), (rA3), (rA4), (rA5), (rA20), (rA29), (rA30), are due to the explanations in [20] or unit consistency. For (rA74),(rA75),(rA76), refer to [26]. The

other errors can be easily seen from the basic conservation principle and the unit consistency.

Acknowledgements

The study was supported, in part, by the grants from Providence University and Taichung Veterans General Hospital (PU-93-11100-5162-006-007) and Taiwan National Science Council (NSC 93-2115-M-126-002- and NSC 94-2115-M-126-002-). Also, we thank the support of the National Center for Theoretical Science (NCTS) of Taiwan.

References

[1] M. Haissaguerre, P. Jais, D. C. Shah, et al, “Spontaneous initiation of atrial fibrillation by ectopic beats originating in the pulmonary veins,” *N Engl J Med*, 339:659-666,1998.

[2] H. Tasaki, “Electrophysiological study of the striated muscle cells of the extrapulmonary vein of the guinea-pig,” *Jpn Circ J*, 33:1087-1098, 1969.

[3] S. A. Chen, Y. J. Chen, H. I. Yeh, C. T. Tai, Y. C. Chen, C. I. Lin, "Pathophysiology of the pulmonary vein as an atrial fibrillation initiator", *Pacing ClinElectrophysion*, 26:1576-1582, 2003-a.

[4] S. A. Chen, C. T. Tai, H. I. Yeh, Y. J. Chen, C. I. Lin, "Controversies in the mechanisms and ablation of pulmonary vein atrial fibrillation", *Pacing ClinElectrophysiol*, 26:1301-1307, 2003-b.

[5] Y. C. Chen, S. A. Chen, Y. J. Chen, M. S. Chang, P. Chan, C. I. Lin, "Effects of thyroid hormone on the arrhythmogenic activity of pulmonary vein cardiomyocytes", *J Am Coll Cardiol*, 39:366-372, 2002-a.

[6] Y. C. Chen, S. A. Chen, Y. J. Chen, C. T. Tai, P. Chan, C. I. Lin, "E®ect of ethanol on the electrophysiological characteristics of pulmonary vein cardiomyocytes", *Eur J Pharmacol*, 483:215-222, 2004-a.

[7] Y. C. Chen, S. A. Chen, Y. J. Chen, C. T. Tai, P. Chen, C. I. Lin, "T-type calcium current in electrical activity of cardiomyocytes isolated from rabbit pulmonary vein", *J Cardiovasc Electrophysiol*, 15:567-571, 2004-b.

[8] Y. J. Chen, S. A. Chen, M. S. Chang, C. I. Lin, "Arrhythmogenic activity of cardiac muscle in pulmonary veins of the dog: implication for the gensesis of atrial fibrillation", *Cardiovasc Res*, 48:265-273, 2000.

[9] Y. J. Chen, S. A. Chen, Y. C. Chen, "Effects of rapid atrial pacing on the arrhythmogenic activity of single cardiomyocytes from pulmonary veins: implication in initiation of atrial fibrillation", *Circulation*, 104:2849-2854, 2001

[10] Y. J. Chen, S. A. Chen, Y. C. Chen, H. I. Yeh, M. S. Chang, C. I. Lin, "Electrophysiology of single cardiomyocytes isolated from rabbit pulmonary veins: implication in initiation of focal atrial fibrillation", *Basic Res Cardiol*, 97:26-34, 2002-b.

[11] Y. J. Chen, Y. C. Chen, P. Chan, C. I. Lin, S. A. Chen, “Temperature regulates the arrhythmogenic activity of pulmonary vein cardiomyocytes,” *J Biomed Sci*, 10:535-543, 2003-c.

[12] Y. J. Chen, Y. C. Chen, H. I. Yeh, C. I. Lin, S. A. Chen, “Electrophysiology and arrhythmogenic activity of single cardiomyocytes from canine superior vena cava,” *Circulation*, 105:2679-2685, 2002-c.

[13] J. R. Ehrlich, T. J. Cha, L. Zhang, D. Charties, P. Melnyk, S. H. Hohnlose, S. Nattel, “Cellular electrophysiology of canine pulmonary vein cardiomyocytes: action potential and ionic current properties,” *J Physiol*, 551:801-813, 2003.

[14] M. Hocini, S. Y. Ho, T. Kawara, et al, “Electrical conduction in canine pulmonary veins: electrophysiological and anatomic correlation,” *Circulation*, 105:2442-2448, 2002.

[15] H. Honjo, M. R. Boyett, R. Niwa, S. lnada, M. Yamamoto, K. Mitsui, T. Horiuchi, N. Shibata, K. Kamiya, I. Kodama, “Pacing-induced spontaneous activity in myocardial sleeves of pulmonary veins after treatment with-ryanodine,” *Circulation*, 107:1937-1943, 2003.

[16] S. S. Po, Y. Li, D. Tang, H. Liu, N. Geng, W. M. Jackman, B. Scherlag, R. Lazzara, E. Patterson, “Rapid and stable re-entry within the pulmonary vein as a mechanism initiating paroxysmal atrial fibrillation,” *Journal of the American College of Cardiology*, 45:1871-1877, 2005.

[17] T. M. Wang, C. E. Chiang, J. R. Sheu, C. H. Tsou, H. M. Chang, H. N. Luk, “Homogenous distribution of fast response action potentials in canine pulmonary vein sleeves: a contradictory report,” *Int J Cardiol*, 89:187-195, 2003.

[18] T. M. Wang, H. N. Luk, J. R. Sheu, H. P. Wu, C. E. Chiang, “Inducibility of abnormal automaticity and triggered activity in myocardial sleeves of canine polmonary veins,” *Int J Cardiol*, 104:59-66, 2005.

[19] A. L. Hodgkin and A. F. Huxley, “A Quantitative Description of Membrane Current and its Application to Conduction and Excitation in Nerve,” J. Physiol, 117:500-544, 1952.

[20] J. Kneller, R. J. Ramirez, D. Chartier, M. Courtemanche, and S. Nattel, “Time-dependent transients in an ionically based mathematical model of the canine atrial action potential,” *Am J Physiol Heart Circ Physiol*, 282: H1437-H1451, 2002.

[21] R. J. Ramirez, S. Nattel and M. Courtemanche, “Mathematical analysis of canine atrial action potentials: rate, regional factors, and electrical remodeling,” *Am J Physiol Heart Circ Physiol*, 279: H1767-H1785, 2000.

[22] D. Li, L. Zhang, J. Kneller and S. Nattel, “Potential ionic mechanism for repolarization differences between canine right and left atrium,” *Circ Res*, 88:1168-1175, 2001.

[23] F. H. Fenton, E. M. Cherry, H. M. Hastings, S J. Evans, “Multiple mechanisms of spiral wave breakup in a model of cardiac electrical activity,” *Chaos*, 12:852-892, 2002.

[24] A. Garfinkel, H. Kim,O. Voroshilovsky, et al., “Preventing ventricular fibrillation by flattening cardiac restitution,” *Proc Natl Acad Sci USA*, 97:6061-6066, 2000.

[25] J. N. Weiss, A. Garfinkel, H. S. Karagueuzian, Z. Qu, P. S. Chen, “Chaos and the transition to ventricular fibrillation: a new approach to antiarrhythmic drug evaluation,” *Circulation*, 99:2819-2826,1999.

[26] J. Keener and J. Sneyd, Mathematical Physiology, in “interdisciplinary Applied Mathematics 8” (J.E. Marsden, L. Sirovich, and S. Wiggins editors), New York, Spinger-Verlag, 1998.